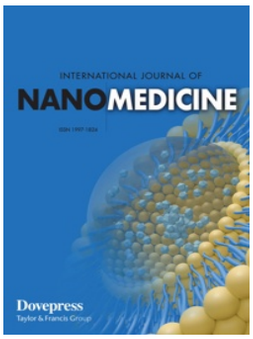

International Journal of Nanomedicine

ISSN: 1176-9114 (Print) 1178-2013 (Online) Journal homepage: www.tandfonline.com/journals/dijn20

Continuous Coagulation Monitoring in Human Blood Samples via Magnetic Particle Spectroscopy

Maria-Josephina Buhné, Justin Ackers, Mandy Ahlborg, Matthias Graeser, Thorsten M Buzug, Kerstin Luedtke-Buzug, Tobias Knopp, Jonas Stroeder, Jörg Barkhausen, Roman Kloeckner, Alex Frydrychowicz, Franz Wegner & Eric Aderhold

To cite this article: Maria-Josephina Buhné, Justin Ackers, Mandy Ahlborg, Matthias Graeser, Thorsten M Buzug, Kerstin Luedtke-Buzug, Tobias Knopp, Jonas Stroeder, Jörg Barkhausen, Roman Kloeckner, Alex Frydrychowicz, Franz Wegner & Eric Aderhold (2026) Continuous Coagulation Monitoring in Human Blood Samples via Magnetic Particle Spectroscopy, International Journal of Nanomedicine, , 561511, DOI: 10.2147/IJN.S561511

To link to this article: https://doi.org/10.2147/IJN.S561511

Published online: 24 Feb 2026.

International Journal of Nanomedicine

Dovepress
Taylor & Francis Group

Open Access Full Text Article

ORIGINAL RESEARCH

Continuous Coagulation Monitoring in Human Blood Samples via Magnetic Particle Spectroscopy

Maria-Josephina Buhné[1,*], Justin Ackers[2,*], Mandy Ahlborg[2], Matthias Graeser[2,3], Thorsten M Buzug[2,4], Kerstin Luedtke-Buzug[4], Tobias Knopp[2,5,6], Jonas Stroeder[1], Jörg Barkhausen[1], Roman Kloeckner[7], Alex Frydrychowicz[1], Franz Wegner[2,7], Eric Aderhold[2]

[1]Institute of Radiology and Nuclear Medicine, University Hospital Schleswig-Holstein, Luebeck, Germany; [2]Fraunhofer IMTE, Fraunhofer Research Institution for Individualized Medical Technology and Engineering, Luebeck, Germany; [3]Chair of Metrology, University of Rostock, Rostock, Germany; [4]Institute of Medical Engineering, University of Luebeck, Luebeck, Germany; [5]Section for Biomedical Imaging, University Medical Center Hamburg-Eppendorf, Hamburg, Germany; [6]Institute for Biomedical Imaging, Hamburg University of Technology, Hamburg, Germany; [7]Institute of Interventional Radiology, University Hospital Schleswig-Holstein, Luebeck, Germany

*These authors contributed equally to this work

Correspondence: Maria-Josephina Buhné, University Hospital-Schleswig-Holstein, Campus Lübeck, Ratzeburger Allee 160, Lübeck, 23538, Germany, Email maria-josephina.buhne@uksh.de; Justin Ackers, Fraunhofer IMTE, Fraunhofer Research Institution for Individualized Medical Technology and Engineering, Mönkhofer Weg 239a, Lübeck, 23562, Germany, Email justin.ackers@imte.fraunhofer.de

Introduction: Magnetic Particle Imaging (MPI) is a radiation-free imaging modality based on the nonlinear magnetic response of iron oxide nanoparticles, providing high sensitivity and real-time, quantitative, background-free imaging. With the clinical approval of Resotran as an MPI-suitable tracer and the development of first human-scale scanners, clinical applications are within reach. Magnetic Particle Spectroscopy (MPS), the non-imaging counterpart of MPI, enables sensitive analytics by exploiting the signal response of magnetic nanoparticles. In this pilot study, we prove the potential of MPS to continuously monitor blood coagulation in real time.

Methods: Blood samples from five volunteers were mixed with the commercial magnetic resonance imaging contrast agent Resotran. The dynamics of the particle signal were assessed in a custom-built MPS-system for a duration of 45 minutes under various conditions, including the presence of anticoagulants (EDTA, Heparin, Citrate) and mechanical stress. The signal amplitude of the fifth harmonic of the MPS was analyzed. To exclude potential thermal effects, the temperature inside the MPS was monitored by using a fiber optic thermometer during the measurements.

Results: All Resotran-containing blood samples showed a signal decrease over time. Samples with anticoagulants exhibited no relevant signal decrease (EDTA, Citrate) or a smaller decrease (Heparin) compared to samples without anticoagulants. Additionally, mechanical stress induced a signal decay in all samples, further indicating the link between the observed MPS signal decay and blood coagulation.

Conclusion: This study shows that continuous monitoring of human blood coagulation via MPS is feasible, making bedside coagulation monitoring in clinical settings a concrete perspective.

Keywords: magnetic particle imaging, blood coagulation, nanoparticles, nanomedicine

Introduction

Magnetic Particle Imaging (MPI) is a tracer-based imaging modality that exploits the non-linear interaction between magnetic nanoparticles (MNP) and both static and time-varying magnetic fields. Its core feature is the background-free measurement and visualization of the spatial distribution of MNP. These MNP are typically superparamagnetic iron oxide nanoparticles. As a radiation-free preclinical imaging technique, MPI shows significant potential for a wide range of clinical applications, such as cardiovascular imaging,[1] the monitoring of endovascular interventions,[2–4] cerebral imaging,[5,6] and cell tracking.[7]

Until recently, a major obstacle to the clinical adoption for human MPI was the lack of a suitable and clinically approved tracer. With the medical approval of the magnetic resonance imaging (MRI) contrast agent Resotran (b.e.imaging GmbH, Germany) on the European market in 2022 the clinical use of MPI became more concrete, as Resotran is also suitable as an MPI tracer.[8]

https://doi.org/10.2147/IJN.S561511
Received: 5 September 2025
Accepted: 22 January 2026
Published: 25 February 2026

Furthermore, first human size scanners have been introduced in the last years[9–11] and the potential of MPI for functional brain mapping is currently being investigated in non-human primates.[12] Together, these developments make the first clinical MPI studies a realistic prospect in the next years. In particular, cardiovascular imaging including perfusion studies[9,12] and the guidance of interventions[13] are imminent. For these scenarios, MPI's volumetric real-time capabilities and its quantitative nature are advantageous.

In addition to morphological information such as stenoses quantification[14] and artifact-free assessment of stent lumina,[4,15] MPI can also include additional contrasts based on the type and physical environment of MNP. By leveraging MNP as nanosensors for the surrounding environment, it opens possibilities for the detection and quantification of various parameters such as temperature, mobility state, size, and viscosity.[16–19] Consequently, this facilitates the differentiation of tissues and the monitoring of biological processes. For example, cerebral hemorrhages can not only be detected and monitored in real-time with multi-contrast MPI, but it is also possible to distinguish between liquid and clotted blood within the hematoma.[20] The multi-contrast capabilities of plain or functionalized MNP as nanosensors are independent of the detection of the spatial distribution, making them equally applicable in Magnetic Particle Spectroscopy (MPS). In MPS the same signal generating fields as in MPI are used but without any spatial resolution and usually for smaller sample volumes resulting in higher sensitivity. This positions MPS as a viable option for a wide range of bioassays and immunoassays that substantially benefit from multi-contrast information but do not need spatial information.[18,19]

In cardiovascular medicine, the monitoring and control of blood coagulation is of utmost importance. Vessel occlusion, for instance, is caused by thrombus formation resulting from blood clotting. Simultaneously, the prevention of thrombosis, particularly following endovascular treatments, is intrinsically linked to the clotting characteristics of the blood. Therefore, for effective therapy and prevention of vascular diseases, a precise monitoring of blood coagulation is essential. A widely clinically established method for monitoring blood clotting during interventions is the activated clotting time (ACT).[21] For this, blood is taken from the patient, mixed with an activator, and measured using a mobile ACT device. Another point of care method is the rotational thromboelastography (ROTEM) and thromboelastography (TEG) which are viscoelastic tests used for the analysis of plasmatic coagulation and fibrolysis.[22] It is primarily used in surgery and intensive care and offers faster detection of abnormalities than traditional blood tests.

We propose an alternative approach using a bedside MPS device. In this method, patient blood samples could be spiked with MNP, either in addition to or instead of the activator. In line with state-of-the-art procedures, patient blood could be drawn directly into a tube pre-filled with the tracer and subsequently analyzed using a bedside device. MPS has previously been shown to be able to predict clot age and organization via estimating the relaxation time of functionalized nanoparticles.[23] In contrast to established laboratory methods and existing MPS studies, our method allows for continuous monitoring of the coagulation dynamics in real-time.

In this pilot study, the potential of MPS for bedside monitoring of blood clotting is demonstrated by coagulation-induced signal changes of the clinically approved tracer Resotran in human blood samples. To confirm coagulation as the primary cause of the observed induced signal changes, we also tested blood samples treated with established anticoagulants. Furthermore, the influence of mechanical stress on detectable signal changes was studied.

Methods

Study Population

Our study population consists of five healthy volunteers (2 female, 3 male), ranging in age from 27 to 39 years.

Blood Samples

We took six blood samples from each volunteer mixing them with different reagents, resulting in six distinct datasets. All samples were then measured in our custom-built bedside **c**ontinuous **h**emostasis **i**nvestigation **m**agnetic **p**article **s**pectrometer ("CHIMPS", Figure 1). The blood samples were taken individually from the median cubital vein using a butterfly needle (Venofix Safety, B. Braun SE, Germany) and measured immediately after collection using the same procedure and timings. An overview of our experimental workflow is shown in Figure 2. In the first set, we analyzed the pure blood samples as a baseline reference (Exp. 0), in all main experiments (I–III) the blood samples were mixed with the clinically approved tracer Resotran.

Figure 1 The used magnetic particle spectrometer "CHIMPS" (foreground) at the bedside in a clinical setting for endovascular interventions (background). The image depicts the anticipated application for continuous monitoring of patient coagulation status.

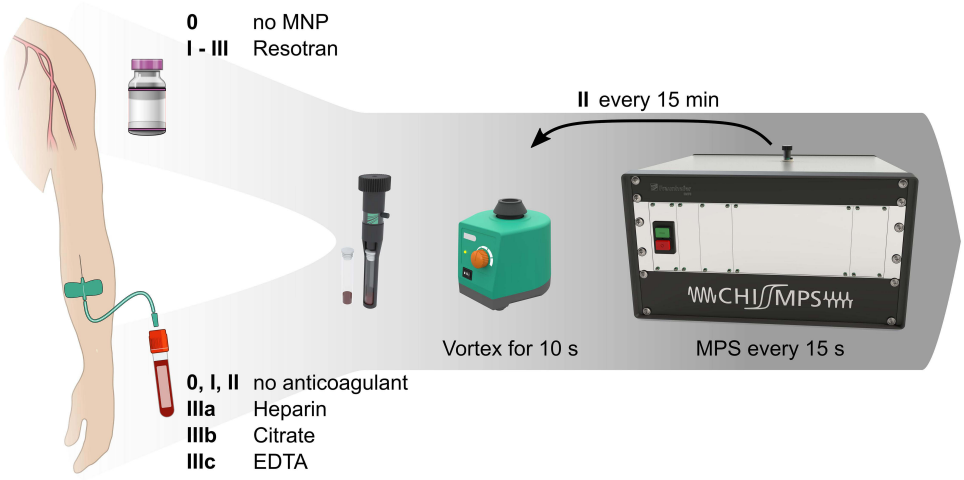

Figure 2 Overview of the experimental sets (0-III), including the investigation of pure (0), Resotran-infused (I), Resotran-infused samples affected by mechanical stress (II) and Resotran-infused samples mixed with anticoagulants (IIIa–IIIc).

From these suspensions, 500 µL samples were prepared with 475 µL blood and 25 µL undiluted Resotran and filled into a soda-lime glass sample tube (ROTILABO 0425.1, Carl Roth GmbH & Co. KG, Germany, 2.5 mL). To ensure homogeneous mixing of the blood samples with all reagents, the samples were vortexed for approximately 10 seconds at ~2000 min^{-1} before insertion into the spectrometer. The initial vortexing was also carried out for the 500 µL pure blood sample to ensure comparability of the results. All samples were then measured continuously in the MPS over a period of 45 minutes.

To investigate the influence of mechanical stress, a known procoagulatory factor, on blood coagulation (Exp. II), an additional blood sample mixed with Resotran was, unlike the other samples, removed from the MPS after 15 and 30 minutes and again vortexed for ~10 s. Subsequently, the measurement was continued as with the other samples (Figure 2).

In addition to mechanical factors, coagulation can also be pharmacologically influenced. Aside from applications during interventions, the use of anticoagulants is widely established in laboratory procedures to inhibit coagulation and preserve samples for later analysis. To test the influence of the most commonly used anticoagulants heparin, citrate and EDTA on the signal of the blood-MNP-mixture (experiments IIIa-c) we used commercial blood collection tubes which were prefilled with these anticoagulants (S-Monovette EDTA K3E, Li Heparin Gel, Citrate 9NC, SARSTEDT AG & Co. KG, Nuembrecht, Germany). Each tube was filled to the intended level to ensure identical concentrations of the anticoagulants. The blood

https://doi.org/10.2147/IJN.S561511

samples were processed as described above. The anticoagulated samples of one female volunteer (F1) were also subjected to mechanical stress, combining the procedures of experiment II and III.

During all measurements, the temperature directly above the sample was monitored using a fiber optic thermometer (FOTEMP-OEM, Weidmann Technologies, Germany). The temperature sensor was not submerged into the sample to not influence the coagulation. While not ideal, a preliminary comparison showed that the temperature above the sample only shows a slight deviation to the temperatures measured inside the suspension.

Tracer Properties and Concentration

Resotran is a clinically approved MRI contrast agent used for the examination of liver lesions. It contains ferucarbotran as iron-oxide nanoparticles, with a saturation magnetization of 83.6 Am^2/kg_{Fe}, a short axis core diameter of 3.3 ± 0.66 nm, and a carboxydextran coating resulting in a hydrodynamic diameter z-average of 66.32 nm.[8] In everyday clinical practice, it is administered in two different dosages depending on the patient's weight. Patients weighing less than 60 kg, receive 0.9 mL and patients weighing more than 60 kg receive 1.4 mL of Resotran (corresponding to 486/756 mg of ferucarbotran or 0.45/0.7 mmol of iron). In contrast to other MRI contrast agents no dose adjustment is necessary in patients with impaired renal or hepatic function. Ferucarbotran is distributed in the intravascular space and rapidly disappears from the blood plasma through selective uptake via the reticuloendothelial system (RES), predominantly in the liver and spleen.[24]

When choosing the tracer concentration, we decided to mimic the bolus concentration used in everyday clinical practice for liver MRI procedures. Typically, a vial of Resotran is diluted with sodium chloride and injected into the patient as a 30 mL bolus. Given the stock concentration of Resotran (28 mg_{Fe}/mL), this equates to a concentration of ~1.4 mg_{Fe}/mL, which was used in this study. This approach ensures that our results are applicable to clinical practices and provides preliminary insights on tracer concentration for use in MPI-MRI hybrid imaging.

Magnetic Particle Spectroscopy

The used custom-built MPS (CHIMPS) operates with a sinusoidal excitation field at 25 kHz, inductively detecting the time-varying non-linear magnetization response of MNPs in the sample.[25] It is encased in an easily transportable 19″ × 6U × 476 mm housing (outer dimensions 520 × 286 × 500 mm; Comptec, Schroff GmbH, Germany), making it suitable for use as both a laboratory and bedside analytical tool.[25] The system has been developed as a modular construction, with a particular focus on the stability and reproducibility of measurements and signal quality, enabling reliable MPS measurements for a wide range of sample geometries. The receive coils used in this study are designed to measure larger volume samples (up to 1 mL) with low concentrations. This feature is especially beneficial when dealing with biological samples, which usually exhibit lower concentrations than undiluted samples used for particle characterization. In essence, the MPS serves as a versatile and efficient analytical tool, ideal for conducting various biological assessments, including blood coagulation tests.

Following the blood sample preparation, all samples were measured in the MPS using the same measurement protocol. Three background measurements without a sample were performed immediately before the experiment and after the finalization of the experiment. After insertion of the blood sample, a single measurement was taken approximately every 15 s for a total of 180 measurement points, resulting in a measurement duration of around 45 minutes per sample. For each point, the excitation field with a frequency of 25 kHz was regulated to 20 mT and the MPS signal was acquired and averaged for 1 s. Their time stamps were used to align the measurements for further analysis.

Data Analysis

The analysis of all recorded data is carried out for each measurement point and is then summarized for the respective experimental sets. For each measurement point, the amplitude of the magnetic moment m at the fifth harmonic is extracted from the transfer function-corrected but not background-corrected single-sided amplitude spectrum.

To describe the captured signal quality and thus the accuracy of the nanosensors as a measuring instrument for the change in the samples, the background signal is calculated in the same way.

The subsequent data analysis is based on the temporal change of the amplitude of the fifth harmonic, which despite the smaller particle signal compared to the third harmonic features the best sensitivity in the used MPS. This is due to the

low thermal noise floor of the receive electronics which make small unstable background signals of the excitation visible in the third harmonic, limiting the sensitivity. However, all odd harmonics featured a qualitatively similar signal trace.

To eliminate the differences in the initial signal amplitudes, all subsequent calculations are made relative to a fixed reference starting point. Particularly at the beginning of the measurements, noticeable temperature variations were observed within the measuring chamber, potentially influencing the particle signal. Therefore, this reference starting point (t_+, m_+) is defined as the amplitude m_+ at the time t_+ when the temperature change between two measuring points is less than 0.1 K ($\sim$7mK/s $\Leftrightarrow$ 0.4K/min).

It can be predicted that the amplitude of the signal will decrease at the stage of coagulation, due to the anticipated restriction in the mobility of the MNP. Consequently, we expect the signal to show a sigmoid curve following the reference starting point.

A variety of points, denoted as tuples of time and amplitude, are selected as characteristic metrics of the observed curves over the measurement time (see Figure 3).

- The first point ($t_{95\%}$, $m_{95\%}$) at which the amplitude, relative to the starting value m_+, has fallen to 95 %, indicating the starting point of the sigmoid curve.
- The second point (t_c, m_c), at the inflection point of the curve, defined by the extremum of the slope and the zero-crossing of the second derivative around this point, as this determines the time at which the change in amplitude decreases over time.
- The final point (t_-, m_-) marking the end point of the observed change was selected as the point at which the change of amplitude between two measurement points is less than 0.5 ‰ of the initial value, indicating that no discernible coagulation effects would be evident in the amplitude by this point.

In experiment II, where the blood samples were additionally exposed to mechanical stress twice, the duration of sample removal and the amplitude change triggered by the applied stress were calculated and expressed as a percentage change ($\Delta t_i^{\downarrow}$, $\Delta m_i^{\downarrow}$). Due to the gaps in the data during the agitation the points $t_{95\%}$ and t_c could not be defined for all samples in this experiment set.

In consideration of minimal amplitude variations observed during utilization of anticoagulants, the signal traces are evaluated using the total signal range over the complete measurement duration $R_m = \max m(t) - \min m(t)$.

Results

Resotran-Infused Blood Samples without Anticoagulants (Experiment I)

In the measurements of the Resotran-infused blood samples (Exp. I), a clear change in MPS signal could be observed over the measurement duration of 45 min (Figure 4). The amplitude of the fifth harmonic of the MPS signal starts at a mean level of 1.19 μAm^2 (SD = 0.03 μAm^2) for all five samples which is nearly stable for around 10 min. After that the signal amplitudes drop following inverted sigmoid shaped curves and on average settle down to 62.1 % of the initial signal level.

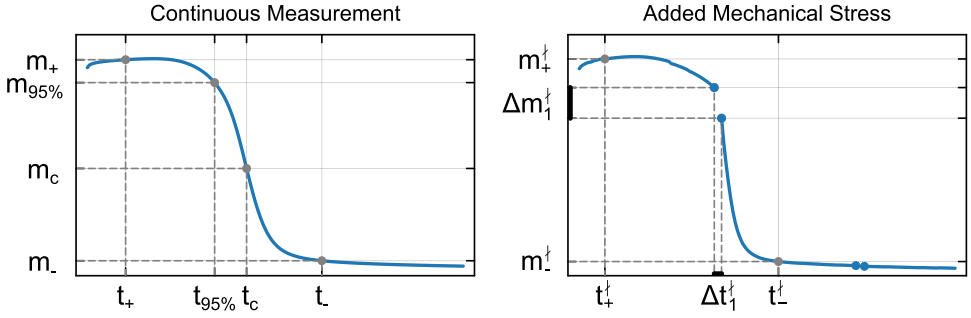

Figure 3 Visualization of the relevant time points and amplitudes extracted from the amplitude curves for further evaluation. For the experiments with induced mechanical, stress the discontinuities in the trace are characterized (right).

https://doi.org/10.2147/IJN.S561511

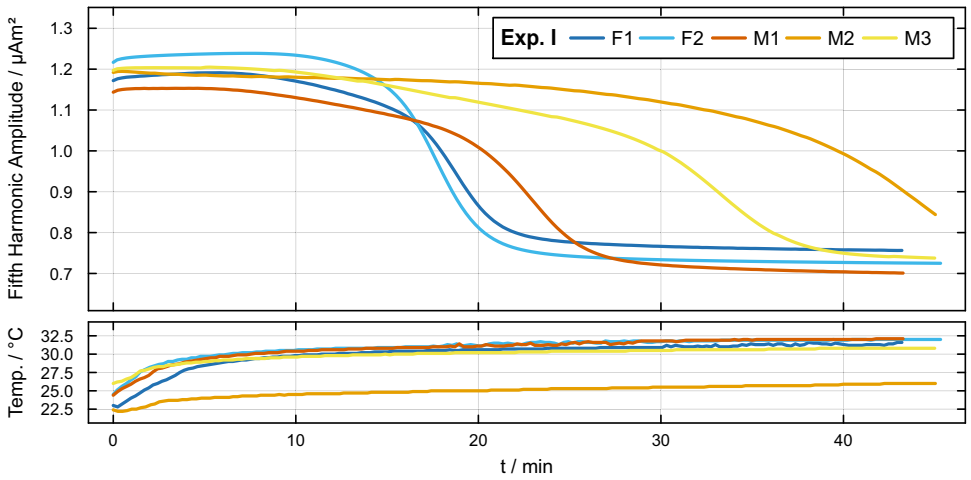

Figure 4 Amplitude traces for the fifth harmonic in the MPS signal from Resotran-infused blood samples (Exp. I) collected from all five volunteers (F: female, M: male), alongside the temperature recorded directly above the sample. All traces exhibit an inverted sigmoid shape with varying timings.

Comparing the minimum signal levels measured in this experiment with the mean signal level of all background measurements (0.0027 μAm^2), reveals a minimal signal-to-noise ratio (SNR) of 255. Considering the mean signal level of 0.0025 μAm^2 in reference experiment 0 for pure blood, it can be assumed that the observed signal variation comes from the interaction of the added MNP with the blood samples and not from an unstable background or the intrinsic signal of the blood itself.

The shape and timing of the inflection point of the curves is characteristic for each sample, with the two female blood samples having the shortest time to their maximum change in signal (see Table 1, t_c). All samples of male volunteers showed both a later point of steepest decline as well as reaching the final plateau later (t_-). For sample M2 the measurement time was too short to capture the complete signal dynamics, and the signal has not reached a stable plateau after 45 minutes. For this measurement, the sample temperature was approximately 5 °C lower than for the other four. It should be noted that the signal traces are not only shifted but also differ in their shape, as samples F2 and M1 have similar $t_{95\%}$ but differ in their t_c by around 5 minutes.

Influence of Mechanical Stress (Experiment II)

With added mechanical stress, the point of the steepest decline is tightly grouped (see. Figure 5), with all samples reaching the final settling point within 10 min after the application of mechanical stress. This is also independent of the

Table 1 Coagulation Curve Metrics for Blood and MNP Suspensions

	t_+	$t_{95\%}$	t_c	t_-	$m_+/\mu Am^2$	m_c	m_-
F1	05:35	13:35	18:54	26:54	1.191	78.5 %	64.8 %
F2	04:16	14:28	17:47	26:12	1.236	78.3 %	59.8 %
M1	04:51	14:34	22:36	32:19	1.153	77.9 %	62.0 %
M2	03:19	28:48	43:30	N/A	1.187	75.3 %	N/A
M3	03:15	17:10	33:07	41:58	1.203	74.8 %	61.7 %
M	04:15	17:43	27:11	31:51	1.19	76.9 %	62.1 %
SD	01:00	06:20	10:56	07:16	0.03	1.8 %	2.0 %

Notes: Overview of the extracted metrics (see Figure 3) of the coagulation curves of the blood and MNP suspension (Exp. I, see Figure 4). The times are expressed in minutes and seconds from the start of the measurement, and the amplitudes are given as a percentage deviation from the reference point m_+. For measurement M2, some values (marked N/A) cannot be provided as the coagulation curve is not fully captured within the measurement time. They are excluded from the descriptive statistics given as mean (M) and standard deviation (SD). Times are given as min:s.

https://doi.org/10.2147/IJN.S561511

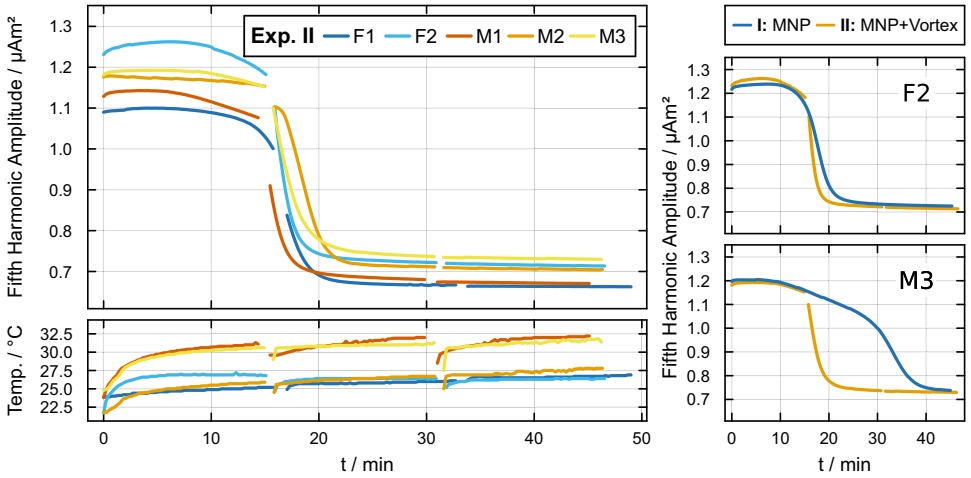

Figure 5 Signal traces for the measurements performed with additional mechanical stress at 15 and 30 min into the analysis (Exp. II, left), and exemplary comparisons with the undisturbed measurements (right; see Figure 4). The data illustrates that the curves follow a qualitatively similar pattern up until the initial mechanical disturbance, after which experiments I and II strongly diverge, while ultimately converging towards a similar amplitude. In the corresponding legend "F" denotes female and "M" denotes male subjects.

sample temperature as two samples had a temperature comparable to experiment I and three had a lower temperature as M2 in experiment I. When comparing the blood samples of identical subjects with and without mechanical stress the initial curve follows the same trajectory until the vortexing at 15 min. After that, the dynamics drastically differ, and the signal settles to the final amplitude substantially earlier ($t_{-}^{\dagger}$ vs t_{-} in Tables 1 and 2). While during the first vortexing the MPS signal is reduced on average by 8.9 % in 59 s, the second application of mechanical stress does only change the signal amplitude by 0.3 %.

Influence of Anticoagulants (Experiments III)

In contrast to the grouping effect of mechanical stress on the observed signal curves, the use of anticoagulants changes the observed signal trace significantly. Figure 6 shows the recorded signal traces for all subjects with blood samples with no anticoagulant (Exp. I) as well as the suspensions with added heparin, citrate, and EDTA (experiments III). The sigmoid shape observed in the previous experiments is only visible in a single trace in the dataset, while all other samples show either no significant change (citrate and EDTA) or a slow drift to an amplitude above the m_{-} level of the traces of experiment II. The quantification of the total signal variation is listed in Table 3. Here, the anticoagulation using citrate

Table 2 Coagulation Curve Metrics of Blood and MNP Suspensions Under Mechanical Stress

	$t_{+}^{\dagger}$	$t_{-}^{\dagger}$	$m_{+}^{\dagger}$ / μAm^2	$m_{-}^{\dagger}$	$\Delta t_{1}^{\dagger}$	$\Delta m_{1}^{\dagger}$	$\Delta t_{2}^{\dagger}$	$\Delta m_{2}^{\dagger}$
F1	02:43	23:24	1.099	61.2 %	01:17	14.8 %	01:06	0.3 %
F2	02:51	22:14	1.256	58.3 %	00:48	6.3 %	00:57	0.2 %
M1	04:36	22:31	1.142	60.3 %	01:06	14.6 %	01:11	0.5 %
M2	03:33	24:24	1.174	61.0 %	00:51	4.4 %	00:50	0.1 %
M3	04:16	24:37	1.192	62.5 %	00:51	4.5 %	00:52	0.2 %
M	03:36	23:26	1.17	60.7 %	00:59	8.9 %	00:59	0.3 %
SD	00:49	01:04	0.06	1.5 %	00:12	5.4 %	00:09	0.2 %

Notes: Overview of the extracted metrics (see Figure 3) from the coagulation curves of blood and MNP suspension influenced by mechanical stress (Exp. II, marked with †, see Figure 5). Times are expressed in minutes and seconds from the start of the measurement, and amplitudes are presented as percentage deviations from the reference point $m_{+}^{\dagger}$. Additionally, the time gap in the measurements and the corresponding amplitude change in percentage points is given. The descriptive statistics are given as mean and standard deviation (M, SD) and times are given as min:s.

https://doi.org/10.2147/IJN.S561511

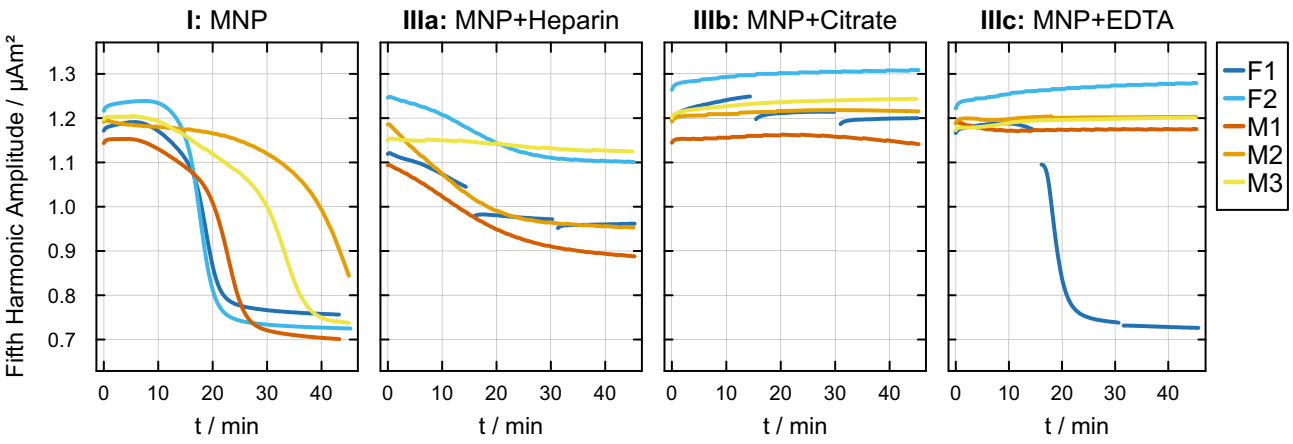

Figure 6 Comparison of the plain blood MNP mixture (Exp. I) with those supplemented with additional anticoagulants (experiments III). In the corresponding legend "F" denotes female and "M" denotes male subjects.

and EDTA achieves similar signal ranges around M = 0.02 µAm^2 and M = 0.03 µAm^2, respectively. The heparin samples vary from subject to subject, with generally larger drifts in the observed MPS signal. Following stabilization, the temperatures inside the sample holder during experiment III were found to be within the range of 24.1 to 32.7 °C. This temperature range was therefore comparable to that of experiment II (Figure 5, bottom).

Discussion

This study demonstrates that the coagulation of human blood, when combined with MNP, induces changes in MPS signals. This highlights the potential of MPS-based coagulation monitoring. The results give insights into blood sample handling and broaden the perspective for the clinical translation of this experimental technique.

We hypothesize that the observed decreases in MPS signal are caused by magnetic relaxation effects induced by viscosity changes of the particle-blood suspension occurring during coagulation. Magnetic relaxation primarily involves two mechanisms: Néel relaxation and Brownian relaxation. The observed signal changes seem to be mainly influenced by Brownian relaxation which describes the physical rotation of the entire nanoparticle within the surrounding fluid to align its magnetic moment with the external magnetic excitation field. Brownian relaxation of the used tracer is known to be affected by matrix viscosity,[26] temperature and nanoparticle configuration.[27] We assume clot formation reduces particle mobility and thus the MPS signal. This is supported by the observation that the signal decay was significantly lower in

Table 3 Coagulation Curve Metrics of Blood and MNP Suspensions with Different Anticoagulants

	I: Pure Suspension $R_m/\mu Am^2$	**IIIa: Suspension plus Heparin** $R_m/\mu Am^2$	**IIIb: Suspension plus Citrate** $R_m/\mu Am^2$	**IIIc: Suspension plus EDTA** $R_m/\mu Am^2$
F1	0.435	0.159	0.062	0.462
F2	0.514	0.138	0.024	0.038
M1	0.452	0.187	0.022	0.013
M2	0.343	0.206	0.012	0.008
M3	0.467	0.027	0.025	0.021
M	0.44	0.14	0.03	0.11 (0.02)
SD	0.06	0.07	0.02	0.2 (0.01)

Notes: Total signal range R_m within the measurement period for different anticoagulants of blood samples with added MNP. The descriptive statistics are presented as the mean (M) and standard deviation (SD). For the experiment with EDTA (Exp. IIIc), the values in parentheses exclude sample F1, as it remarkably differs from the other measurements in the set.

blood samples mixed with anticoagulants. Nevertheless, the non-zero signal after the clotting can be attributed to the persistent Néel relaxation.

The dependency between particle signal and viscosity of the surrounding medium was described in previous studies that have shown the potential of MPI for temperature and viscosity mapping.[16,17] Hence, multi-contrast MPI allows the discrimination of MNP with different signal properties.[28] The observed variance in the initial amplitudes of the different samples can most likely be attributed to inaccuracies in the MNP concentration, however, it cannot be ruled out that the initial viscosity of the subjects' blood samples already influenced the initial signal amplitude.

There are several factors that can influence blood coagulation and thus the MPS signal of blood-MNP-mixtures. In the present dataset, the shortest coagulation times are observed in the samples from the two female volunteers as measured by both the inflection point as well as the final settling point. This aligns with the general trend of higher coagulation potential in women.[29] However, our cohort is too small to draw a conclusion.

Additionally, mechanical stress such as shaking is a procoagulatory factor.[30] Our experiments align with that, as all samples showed a rapid signal decrease and harmonization of the curves after mechanical stress induced by vortexing. This implies a swift acceleration of coagulation due to mechanical factors. It presents compelling evidence that the signal discrepancies observed in this study are indeed attributable to coagulation. Furthermore, the prevention of mechanical stress is essential regarding the handling of blood samples for any coagulation analysis method.[31]

Another factor that affects blood clotting is the sample temperature. Low temperatures slow down blood clotting via a platelet adhesion defect and reduced enzyme activity.[32] Aside from the sex-specific differences mentioned above, this is one probable cause for the delayed coagulation response observed in the signal curve of subject M2 in experiment I, as the sample temperature was 5 K lower compared to the other samples. Not only are the coagulation properties influenced by different temperatures, but the signal behavior of MNP is also temperature dependent. Utkur et al introduced the possibility of relaxation-based temperature mapping with MPI,[17] which is e.g. beneficial for ablation procedures.[33] Therefore, temperature differences are an important influencing variable for the anticipated MPS-based anticoagulation monitoring, indicating the need for a temperature-controlled measurement device and careful sample handling.

In interventional scenarios, the use of anticoagulants is crucial to prevent thrombosis. Therefore, the possibility to monitor the coagulation status of the blood mixed with anticoagulants is essential. In our experiments, the samples anticoagulated with citrate and EDTA were missing the previously observed sigmoid curve shape, indicating a potential effective anticoagulation monitoring using the MPS signal. In contrast, most samples with heparin show a clear signal decrease during the measurement time. We assume this to be caused by different resulting mixing ratios of the blood with the anticoagulants. Heparin is contained as small drug-coated beads in the sample tube, while EDTA and citrate are present liquid in the corresponding tubes. Maybe the fluid components mixed up better with the blood than the solid beads. Nevertheless, we cannot strictly rule out any molecular interactions between the nanoparticles and heparin, which might influence the resulting MPS signal.

To test whether mechanical stress also leads to signal changes in the anticoagulated samples we mechanically stressed the anticoagulated sample tubes of one female test subjects by a vortex machine, as in the previous experiment on mechanical stress. The samples with heparin and citrate showed no difference compared to the samples of the other subjects, except for the temperature induced amplitude deviations after the reinsertion of the samples. However, in the sample with EDTA there was a clear signal drop after application of mechanical stress. We assume this to be a measurement error, while other possible explanations could include EDTA-induced platelet aggregation, which rarely occurs. An alternative hypothesis might be the disturbance of EDTA-induced complex formation due to mechanical stress.[34]

The results of this work have strong translational potential for patient care, due to the clinical approval of the used tracer agent, the bedside capable setup of CHIMPS, with its wipeable surface and silent operation, and the used human blood samples. Continuous bedside coagulation monitoring is especially interesting in the context of intensive care units and endovascular interventional procedures. Here, it could be highly beneficial to detect disturbances of blood coagulation very early. This is of high clinical importance, as bleeding or thrombotic events can effectively be prevented. In clinical routine coagulation parameters are determined by time intensive laboratory analyses and by determining the "activated clotting time" in the operation room. The latter is a possibility which allows for coagulation monitoring with a latency of minutes. In contrast the advantage of our method is the possibility to monitor the coagulation process continuously, in real-time with very high

accuracy also including parameters that can be extracted from the shape of the continuous signal curve. While both ROTEM and PEG also allow for dynamic assessment of the coagulation process, they function by applying continuous macroscopic forces to the sample, thereby influencing the coagulation process. MPS seemingly exerts minimal mechanical stress on the sample due to the negligible forced movement of the nanoparticles, which may consequently unveil further coagulation dynamics. Furthermore, functionalized MNP e.g. with antibodies,[35] allow for specific tests beyond coagulation in general. Assuming an already established clinical MPI application, it would also be conceivable that the blood taken could be examined directly without having to be mixed with a further reagent, provided an MNP-based contrast agent is already administered for an MPI-guided intervention.

Our study has several limitations which need to be discussed. The MPS, which was used in this study, is not approved as a medical device so far and environmental tests to prove robust performance in a clinical environment with electromagnetic noise are still pending. Furthermore, the sample size of five volunteers and the homogeneous age distribution among them limits the transferability of the results to the general population. Additionally, a ground truth of the volunteers' coagulation status is missing in this pilot study. Therefore, we cannot quantify the effects of blood coagulation we observed. Furthermore, we cannot exclude the initial vortexing of the blood samples to ensure homogeneous mixing with the SPIONs served as a coagulation inductor. In that regard, swinging of the sample should be investigated as an alternative approach to vortexing. The coagulation might also have been influenced by temperature effects due to the ex vivo transfer of the samples to the MPS, a standard procedure with clinically approved blood analysis devices, and temperature effects in the measuring chamber itself. In the future this could be improved by adding a temperature stabilized sample holder, which could be included in the current MPS design due to the modular system. During the processing of the MPS signals it might be beneficial to also include phase information in addition to the amplitudes used in this study, further increasing sensitivity to environmental changes of the MNPs. Furthermore, we have only tested a single type of nanoparticles which may limit the generalizability of the results to other particle entities. Additionally, the effect of SPIONs on coagulation, e.g. through the contact pathway, should be investigated. In future work a comprehensive validation of the MPS measurements is imperative, alongside a systematic comparison with existing methodologies and devices. The employment of standardised clinical assays is vital for the quantification of observed effects, thus facilitating an evidence-based comparison of performance and clinical utility.

In conclusion, our study proves that the coagulation of human blood can be monitored continuously by means of MPS. This makes bedside real-time coagulation monitoring in medical environments potentially feasible. The diverse effects of different anticoagulants, along with mechanically induced coagulation, provide important insights into sample handling for analytical MPS applications using patient blood.

Data Sharing Statement

The datasets used and/or analyzed during the current study are available from the corresponding author Justin Ackers on reasonable request.

Ethics Approval

This experimental pilot study was approved by the local ethics committee of the University of Luebeck, Germany (approval no. 2024-176_2). Our study complies with the declaration of Helsinki. Informed consent was obtained from the study participants prior to study commencement.

Consent for Publication

Consent for publication was obtained from all authors.

Author Contributions

All authors made a significant contribution to the work reported, whether that is in the conception, study design, execution, acquisition of data, analysis and interpretation, or in all these areas; took part in drafting, revising or critically reviewing the article; gave final approval of the version to be published; have agreed on the journal to which the article has been submitted; and agree to be accountable for all aspects of the work.

All authors approved the final version of the manuscript.

Funding

This work partially was funded by the University of Lübeck (LACS04-2025), the EU (EFRE) and the State Schleswig-Holstein (Projects: IMTE 1+2 – Grant: LPW-E1.1.1/1536, 124 20 002 and LPW21-L/2.2/262, 125 24 009).

Disclosure

Prof. Dr. Roman Kloeckner reports personal fees from consulting fees from Boston Scientific, Bristol Myers Squibb, Guerbet, Roche, and Sirtex and lecture fees from Astra Zeneca, BTG, Eisai, Guerbet, Ipsen, Roche, Siemens, Sirtex, MSD Sharp & Dohme, non-financial support from Chair of the Audit and Standards Subcommittee of the European Society of Radiology, outside the submitted work. All authors declare no competing interests.

References

1. Weizenecker J, Gleich B, Rahmer J, Dahnke H, Borgert J. Three-dimensional real-time in vivo magnetic particle imaging. *Phys Med Biol*. 2009;54 (5):L1–L10. doi:10.1088/0031-9155/54/5/L01
2. Herz S, Vogel P, Dietrich P, et al. Magnetic particle imaging guided real-time percutaneous transluminal angioplasty in a phantom model. *Cardiovasc Intervent Radiol*. 2018;41(7):1100–1105. doi:10.1007/s00270-018-1955-7
3. Haegele J, Rahmer J, Gleich B, et al. Magnetic particle imaging: visualization of instruments for cardiovascular intervention. *Radiology*. 2012;265 (3):933–938. doi:10.1148/radiol.12120424
4. Wegner F, Friedrich T, von Gladiss A, et al. Magnetic particle imaging: artifact-free metallic stent lumen imaging in a phantom study. *Cardiovasc Intervent Radiol*. 2020;43(2):331–338. doi:10.1007/s00270-019-02347-x
5. Orendorff R, Peck AJ, Zheng B, et al. First in vivo traumatic brain injury imaging via magnetic particle imaging. *Phys Med Biol*. 2017;62 (9):3501–3509. doi:10.1088/1361-6560/aa52ad
6. Ludewig P, Gdaniec N, Sedlacik J, et al. Magnetic particle imaging for real-time perfusion imaging in acute stroke. *ACS Nano*. 2017;11 (10):10480–10488. doi:10.1021/acsnano.7b05784
7. Bulte JWM, Walczak P, Janowski M, et al. Quantitative "Hot Spot" imaging of transplanted stem cells using superparamagnetic tracers and Magnetic Particle Imaging (MPI). *Tomogr J Imaging Res*. 2015;1(2):91–97. doi:10.18383/j.tom.2015.00172
8. Mohn F, Scheffler K, Ackers J, et al. Characterization of the clinically approved MRI tracer resotran for magnetic particle imaging in a comparison study. *Phys Med Biol*. 2024;69(13):135014. doi:10.1088/1361-6560/ad5828
9. Graeser M, Thieben F, Szwargulski P, et al. Human-sized magnetic particle imaging for brain applications. *Nat Commun*. 2019;10(1):1936. doi:10.1038/s41467-019-09704-x
10. Vogel P, Rückert MA, Greiner C, et al. iMPI: portable human-sized magnetic particle imaging scanner for real-time endovascular interventions. *Sci Rep*. 2023;13(1):10472. doi:10.1038/s41598-023-37351-2
11. Mattingly E, Sliwiak M, Mason EE, et al. Design, construction and validation of a magnetic particle imaging (MPI) system for human brain imaging. *Phys Med Biol*. 2024. doi:10.1088/1361-6560/ad9db0
12. Barksdale AC, Niebel FH, Chacon-Caldera J, et al. Measurement of cerebral blood volume modulation in non-human primates. *Int J Magn Part Imaging*. 2025;11(1 Suppl 1). doi:10.18416/IJMPI.2025.2503029
13. Hartung V, Gruschwitz P, Augustin AM, et al. Magnetic particle imaging angiography of the femoral artery in a human cadaveric perfusion model. *Commun Med*. 2025;5(1):75. doi:10.1038/s43856-025-00794-x
14. Vaalma S, Rahmer J, Panagiotopoulos N, et al. Magnetic Particle Imaging (MPI): experimental quantification of vascular stenosis using stationary stenosis phantoms. *PLoS One*. 2017;12(1):e0168902. doi:10.1371/journal.pone.0168902
15. Wegner F, von Gladiss A, Haegele J, et al. Magnetic particle imaging: in vitro signal analysis and lumen quantification of 21 endovascular stents. *Int J Nanomed*. 2021;16:213–221. doi:10.2147/IJN.S284694
16. Utkur M, Muslu Y, Saritas EU. Relaxation-based viscosity mapping for magnetic particle imaging. *Phys Med Biol*. 2017;62(9):3422–3439. doi:10.1088/1361-6560/62/9/3422
17. Utkur M, Saritas EU. Simultaneous temperature and viscosity estimation capability via magnetic nanoparticle relaxation. *Med Phys*. 2022; mp.15509. doi:10.1002/mp.15509
18. Wu K, Liu J, Chugh VK, et al. Magnetic nanoparticles and magnetic particle spectroscopy-based bioassays: a 15 year recap. *Nano Futur*. 2022;6 (2):022001. doi:10.1088/2399-1984/ac5cd1
19. Wu K, Su D, Saha R, Liu J, Chugh VK, Wang JP. Magnetic particle spectroscopy: a short review of applications using magnetic nanoparticles. *ACS Appl Nano Mater*. 2020;3(6):4972–4989. doi:10.1021/acsanm.0c00890
20. Szwargulski P, Wilmes M, Javidi E, et al. Monitoring intracranial cerebral hemorrhage using multicontrast real-time magnetic particle imaging. *ACS Nano*. 2020;14(10):13913–13923. doi:10.1021/acsnano.0c06326
21. Hoebink M, Steunenberg TAH, Roosendaal LC, et al. Ability of activated clotting time measurements to monitor unfractionated heparin activity during noncardiac arterial procedures. *Ann Vasc Surg*. 2025;110:460–468. doi:10.1016/j.avsg.2024.10.003
22. Whiting D, DiNardo JA. TEG and ROTEM: technology and clinical applications. *Am J Hematol*. 2014;89(2):228–232. doi:10.1002/ajh.23599
23. Khurshid H, Shi Y, Berwin BL, Weaver JB. Evaluating blood clot progression using magnetic particle spectroscopy. *Med Phys*. 2018;45 (7):3258–3263. doi:10.1002/mp.12983
24. Summary of Product Characteristics: Resotran 540 mg/mL suspension for injection. Available from: https://docetp.mpa.se/LMF/Resotran%20suspension%20for%20injection%20ENG%20SmPC_09001bee82978192.pdf. Accessed December 15, 2025.
25. Aderhold E, Ackers J, Stagge P, et al. Development and Assessment of a 1D-MPS. *Int J Magn Part Imaging*. 2025;11(1 Suppl 1). doi:10.18416/IJMPI.2025.2503056

26. Goto H, Futagawa M, Takemura Y, Ota S. Effects of Néel and Brownian relaxations on dynamic magnetization empirically characterized in single-core and multicore structures of magnetic nanoparticles. *Nanoscale*. 2025;17(20):12817–12825. doi:10.1039/D5NR00722D
27. Ota S, Takemura Y. Characterization of Néel and Brownian relaxations isolated from complex dynamics influenced by dipole interactions in magnetic nanoparticles. *J Phys Chem C*. 2019;123(47):28859–28866. doi:10.1021/acs.jpcc.9b06790
28. Rahmer J, Halkola A, Gleich B, Schmale I, Borgert J. First experimental evidence of the feasibility of multi-color magnetic particle imaging. *Phys Med Biol*. 2015;60(5):1775–1791. doi:10.1088/0031-9155/60/5/1775
29. Gorton HJ, Warren ER, Simpson NAB, Lyons GR, Columb MO. Thromboelastography identifies sex-related differences in coagulation. *Anesth Analg*. 2000;91(5):1279–1281. doi:10.1213/00000539-200011000-00042
30. Miyazaki Y, Nomura S, Miyake T, et al. High shear stress can initiate both platelet aggregation and shedding of procoagulant containing microparticles. *Blood*. 1996;88(9):3456–3464. doi:10.1182/blood.V88.9.3456.bloodjournal8893456
31. Kitchen S, Adcock DM, Dauer R, et al. International Council for Standardization in Haematology (ICSH) recommendations for processing of blood samples for coagulation testing. *Int J Lab Hematol*. 2021;43(6):1272–1283. doi:10.1111/ijlh.13702
32. Wolberg AS, Meng ZH, Monroe DM, Hoffman M. A systematic evaluation of the effect of temperature on coagulation enzyme activity and platelet function. *J Trauma Inj Infect Crit Care*. 2004;56(6):1221–1228. doi:10.1097/01.TA.0000064328.97941.FC
33. Salamon J, Dieckhoff J, Kaul MG, et al. Visualization of spatial and temporal temperature distributions with magnetic particle imaging for liver tumor ablation therapy. *Sci Rep*. 2020;10(1):7480. doi:10.1038/s41598-020-64280-1
34. Banfi G, Salvagno GL, Lippi G. The role of ethylenediamine tetraacetic acid (EDTA) as in vitro anticoagulant for diagnostic purposes. *Clin Chem Lab Med*. 2007;45(5). doi:10.1515/CCLM.2007.110
35. Tomitaka A, Arami H, Gandhi S, Krishnan KM. Lactoferrin conjugated iron oxide nanoparticles for targeting brain glioma cells in magnetic particle imaging. *Nanoscale*. 2015;7(40):16890–16898. doi:10.1039/c5nr02831k